Controlled Growth/Patterning of Ni Nanohoneycombs on Various Desired Substrates

Gaixia Zhang, Shuhui Sun, Mihnea Ioan Ionescu, Hao Liu, Yu Zhong, Ruying Li, and Xueliang Sun*

Department of Mechanical and Materials Engineering, The University of Western Ontario, London, Ontario, N6A 5B9, Canada

We report a two-step process for the growth/patterning of Ni honeycomb nanostructures on various substrates, such as carbon paper, carbon nanotubes (CNTs), silicon wafers, and copper grids, via the combination of a sputter-coating/patterning technique and a replacement reaction solution method. The morphology, crystallinity, and chemical composition of the honeycombs were analyzed by SEM, TEM, high-resolution TEM, and EDX. These honeycombs are composed of numerous nanocells, several tens of nanometers in diameter and with cell wall thickness of ~10 nm, randomly connecting to each other. The growth process of honeycomb nanostructures has been systematically studied. Interestingly, the diameter and wall thickness of the cells could be easily tuned by simply adjusting the experimental parameters, such as the concentrations and cations of metal salts. Additionally, this simple method has been successfully extended to synthesize Co nanostructures with well-controlled morphologies, which indicates the great potential of this strategy in the synthesis of other metal nanostructures on various desired substrates. These metal−substrate composites, especially with desired patterns, are expected to be ideal candidates for wide application in modern electronic and optoelectronic devices, sensors, fuel cells, and energy storage systems.

1. Introduction

Over the past few decades, metal nanostructures have been extensively studied because of their intriguing optical, electronic, and catalytic properties, as well as their wide applications in many fields.[1−5] Accordingly, considerable efforts has been made for the size- and shape-controlled synthesis of various metal nanostructures, such as crystals, wires, tubes, hollow spheres, and so on.[6−9] However, most of them mainly focused on the fabrication of free-standing metal nanostructures. Few studies on the synthesis of metal nanostructures on solid substrate surfaces and even fewer demonstrations for patterned metal nanostructures have been reported so far. Thus, morphology-controlled synthesis of metal nanostructures on desired substrates, especially with patterned forms, is of much scientific and technological interest and can be used to catering to the specific applications in electronics, sensors, and fuel cells.

In recent years, some effort has been made on the synthesis of metal−substrate composites.[10−13] Most progress has focused on the deposition of metal films or patterns that were composed of numerous nanoparticles, by evaporation in a high vacuum system, or via various lithographic techniques.[10,11,14] While these methods have the capability to make a very uniform nanoparticle film, coating the substrates with various nanostructures rather than only nanoparticles may have many more applications since the morphology (including dimensionality and shape) of the nanostructures can effectively tune their intrinsic chemical and physical properties.[15,16] On the other hand, solution methods have been demonstrated as a powerful technique for effective synthesis of various nanostructures. Very recently, Xia et al. demonstrated the success of growing Pt nanowires on ceramic and polymeric microbeads, Pt and W meshes, as well as silicon wafer.[12,17,18] In addition, Wang et al. reported creating Cu metallic-nanowire arrays by corner-mediated electrodeposition.[13] Although progress has been made in the past few years with respect to the procedures, materials used, and numbers of metal nanomaterials that can be synthesized, the production of various ideal metal−substrate composites is still complex, costly, and far from satisfying various application requirements.

Here, based on a replacement reaction, we report, for the first time, a two-step method for the growth/patterning of Ni nanohoneycombs on various substrates, such as carbon paper, carbon nanotubes (CNTs), silicon wafers with and without patterns, and copper grids. These substrates, either conductive or semiconductive, with different morphologies and sizes, are carefully selected, since they are already popular matrices in various fields.

*E-mail: xsun@eng.uwo.ca.
(1) Sun, S. H.; Jaouen, F.; Dodelet, J. P. *Adv. Mater.* **2008**, *20*, 3900–3904.
(2) Guo, Y. G.; Hu, J. S.; Wan, L. J. *Adv. Mater.* **2008**, *20*, 2878–2887.
(3) Chen, S. W.; Yang, Y. Y. *J. Am. Chem. Soc.* **2002**, *124*, 5280–528.
(4) Krasteva, N.; Besnard, I.; Guse, B.; Bauer, R. E.; Mullen, K.; Yasuda, A.; Vossmeyer, T. *Nano Lett.* **2002**, *2*, 551–555.
(5) Taton, T. A.; Mirkin, C. A.; Letsinger, R. L. *Science* **2000**, *289*, 1757–1760.
(6) Xia, Y.; Xiong, Y.; Lim, B.; Skrabalak, S. E. *Angew. Chem., Int. Ed.* **2009**, *48*, 60–103.
(7) Sun, S. H.; Yang, D. Q.; Villers, D.; Zhang, G. X.; Sacher, E.; Dodelet, J. P. *Adv. Mater.* **2008**, *20*, 571.
(8) Liang, H. W.; Liu, S.; Gong, J. Y.; Wang, S. B.; Wang, L.; Yu, S. H. *Adv. Mater.* **2009**, *21*, 1850–1854.
(9) Liang, H. P.; Zhang, H. M.; Hu, J. S.; Guo, Y. G.; Wan, L. J.; Bai, C. L. *Angew. Chem., Int. Ed.* **2004**, *43*, 1540–1543.
(10) Ma, Y.; Wong, C. P.; Zeng, X. T.; Yu, T.; Zhu, Y.; Shen, Z. X. *J. Phys. D: Appl. Phys.* **2009**, *42*, 065417.
(11) Shin, H.; Kim, H.; Lim, K.; Lee, M. *Thin Slolid Films* **2009**, *517*, 3273–3275.
(12) Lee, E. P.; Chen, J.; Yin, Y. Y.; Campbell, C. T.; Xia, Y. *Adv. Mater.* **2006**, *18*, 3271–3274.
(13) Zhang, B.; Weng, Y.; Huang, X.; Wang, M.; Peng, R.; Ming, N.; Yang, B.; Lu, N.; Chi, L. *Adv. Mater.* **2009**, *21*, DOI: 10.1002/adma.200900730.
(14) Zhang, G. X.; Yang, D. Q.; Sacher, E. *J. Phys. Chem. C* **2007**, *111*, 17200–17205.
(15) Wang, Y.; Becker, M.; Wang, L.; Liu, J.; Scholz, R.; Peng, J.; Gösele, U.; Christiansen, S.; Kim, D. H.; Steinhart, M. *Nano Lett.* **2009**, *9*, 2384–2389.
(16) Schwanecke, S.; Fedotov, V. A.; Khardikov, V. V.; Prosvirnin, S. L.; Chen, Y.; Zheludev, N. I. *Nano Lett.* **2008**, *8*, 2940–2943.
(17) Lee, E. P.; Peng, Z.; Cate, D. M.; Yang, H.; Campbell, C. T.; Xia, Y. *J. Am. Chem. Soc.* **2007**, *129*, 10634–10635.
(18) Lee, E. P.; Xia, Y. *Nano Res.* **2008**, *1*, 129–137.

Typically, a thin layer of metal film/patterning to be used as sacrificial metal is sputtered on a desired substrate first, and then the substrate is immersed in a desired metal salt solution to obtain the desired metal−substrate composite. By combining the sputtering and solution techniques, this strategy has the following advantages. (1) It is a simple, controllable, repeatable, cost-effective, and green method. (2) The driving force are mainly controlled by the electrical potential difference between two metals as well as the metal salt precursors; thus, the number of controlled structures that can be obtained using this strategy is potentially very large.[19] (3) The metal nanostructures obtained are very uniform owing to the sacrificial-metal-film uniformity via sputtering.[20,21] (4) The synthesis of patterned metal nanostructures is highly feasible thanks to the successful techniques, such as sputtering, photo, or e-beam/ion beam lithography, microcontact printing, and others that are widely used for the fabrication of patterned nanoparticle films that, in our case, can serve as the sacrificial metals.[22−25] This method is of much interesting because it is simple, cost-effective, and can be extended to realize the growth/patterning of other metal nanostructures on various desired substrates. Further, it is also of scientific and technical significance because modern electronics and optoelectronic devices, chemical sensors, and catalytic systems commonly require nanostructured metallization coating/patterns.[26−29]

2. Experimental Section

Materials and Supplies. Doubly distilled deionized (DI) water was used for all preparations. Nickel(II) chloride hexahydrate ($NiCl_2 \cdot 6H_2O$), nickel(II) nitrate hexahydrate ($Ni(NO_3)_2 \cdot 6H_2O$), cobalt(II) chloride hexahydrate ($CoCl_2 \cdot 6H_2O$), and cobalt(II) nitrate hexahydrate ($Co(NO_3)_2 \cdot 6H_2O$) were obtained from Sigma-Aldrich and used as received. Carbon paper (0.17 mm thick, 81% porosity) were obtained from E-TEK. Carbon nanotubes (CNTs) were in-house synthesized by chemical vapor deposition (CVD) method. Cu grids (100 mesh), acting as a sputtering mask, were obtained from Electron Microscopy Science. Aluminum films, with different thicknesses (e.g., 30 and 100 nm), on various substrates, were prepared using a radio frequency magnetron sputtering device, which is mounted in a plasma-enhanced chemical vapor deposition (PECVD) system. The Al thickness was monitored by a quartz crystal microbalance.

Honeycomb Synthesis. In a typical synthesis, a piece of carbon paper with an aluminum film of a certain thickness (e.g., 30 nm) was immersed in a desired metal salt solution (e.g., $NiCl_2$, 0.1 M), where the atomic concentration of Ni was greater than that of Al so that the Al could be completely consumed, forming Ni nanostructures only. The reaction was conducted at room temperature in ambient atmosphere for 2 days. After the reaction was complete, the metal−substrate composite was washed several times in DI water and dried at room temperature.

Materials Characterization. The morphology, crystallinity, and chemical composition of the samples were determined by
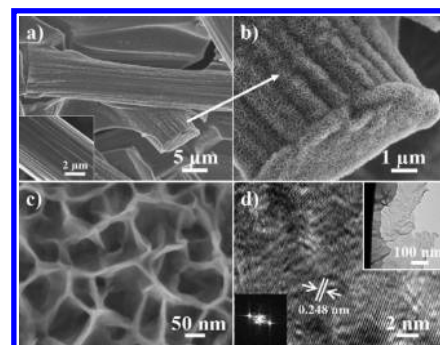

Figure 1. Ni honeycombs synthesized from the reaction of 30 nm Al film on carbon paper and 0.1 M $NiCl_2$ solution. (a,b,c) SEM images; the inset in (a) shows an image of a pristine carbon fiber. (d) HRTEM image; the inset in the upper right corner shows a general TEM image of the honeycombs grown on a carbon fiber, while the inset in the lower left corner shows a FFT which was taken from the lower part of the HRTEM image in (d).

filed-emission scanning electron microscope (FESEM, Hitachi S-4800, operating at 5 kV) equipped with an energy-dispersive X-ray spectrometer (EDX), and high-resolution transmission electron microscope (HRTEM, JEOL 2010F, operating at 200 kV).

3. Results and Discussion

In a typical synthesis, the carbon paper substrate sputtered with an aluminum film in a certain thickness (e.g., 30 nm) was immersed in the desired metal salt solution (e.g., $NiCl_2$, 0.1 M) for two days. The pristine carbon paper substrate is fabricated from small graphite fibers with diameters between 5 and 10 μm (inset in Figure 1a). The low-magnification SEM image (Figure 1a,b) indicates that very uniform Ni honeycomb nanostructures are formed, tightly covering the entire carbon paper surface even over the cross section of broken carbon fibers. The Ni film undulates over the roughness of the pristine carbon fiber surface, indicating the uniform thickness distribution of Ni honeycombs. The EDX spectrum (Supporting Information Figure S1b) shows the purity of the Ni honeycombs. The high-magnification SEM image (Figure 1c) shows the detailed honeycomb structures, composed of numerous cells, 80−100 nm in diameter and with cell wall thickness of ∼10 nm, randomly connecting to each other. The TEM image (inset in Figure 1d) shows that the honeycombs are 150−400 nm tall and made from flat and thin nanosheets, although they sometimes randomly bend or overlap. A high-resolution TEM image (HRTEM, Figure 1d) with visible lattice fringes and the corresponding fast Fourier transformation (FFT) (inset, taken from the lower part of the image) further confirm that the nanosheets are single crystalline. The 0.248 nm lattice spacing matches the interplanar separation of the (110) planes of fcc crystalline Ni.

For a complete view of the honeycomb formation process and its growth mechanism, a morphological evolution study was conducted over an extended period of time at room temperature. Products were collected as a function of reaction time, and their morphologies were evaluated by SEM (Supporting Information Figure S2). Supporting Information Figure S2a,a′ show the morphology of the original Al film, sputtered on a carbon fiber surface, which is densely composed of numerous Al nanoparticles with diameters of about 50 nm. When a sample is collected after 30 min of reaction, the Al nanoparticle surfaces become very rough (Supporting Information Figure S2b,b′), decorated with many tiny Ni buds. After 1 h, on sacrificing Al atoms, Al nanoparticles become obviously smaller; meanwhile, small ridge-like

(19) Bansal, V.; Jani, H.; Plessis, J. D.; Coloe, P. J.; Bhargava, S. K. *Adv. Mater.* **2008**, *21*, 717–723.
(20) Yoon, K. H.; Choi, J. W.; Lee, D. H. *Thin Solid Films* **1997**, *302*, 116–121.
(21) Li, M.; Chokshi, N.; DeLeon, R. L.; Tompa, G.; Anderson, W. A. *Thin Solid Films* **2007**, *515*, 7357–7363.
(22) Cui, Y.; Björk, M. T.; Liddle, J. A.; Sönnichsen, C.; Boussert, B.; Alivisatos, A. P. *Nano Lett.* **2004**, *4*, 1093–1098.
(23) Corvierre, M. K.; Beerens, J.; Beauvais, J.; Lennox, R. B. *Chem. Mater.* **2006**, *18*, 2628–2631.
(24) Chen, J. Y.; Mela, P.; Möller, M.; Lensen, M. C. *ACS Nano* **2009**, *3*, 1451–1456.
(25) Santhanam, V.; Andres, R. P. *Nano Lett.* **2004**, *4*, 41–44.
(26) Shankar, S. S.; Rizzello, L.; Cingolani, R.; Rinaldi, R.; Pompa, P. P. *ACS Nano* **2009**, *3*, 893–900.
(27) Kim, H.; Shin, H.; Ha, J. M.; Lee, M. *J. Appl. Phys.* **2007**, *102*, 083505.
(28) Hamann, H. F.; Woods, S. I.; Sun, S. H. *Nano Lett.* **2003**, *3*, 1643–1645.
(29) Jacobs, H. O.; Whilesides, G. M. *Science* **2001**, *291*, 1763–1766.
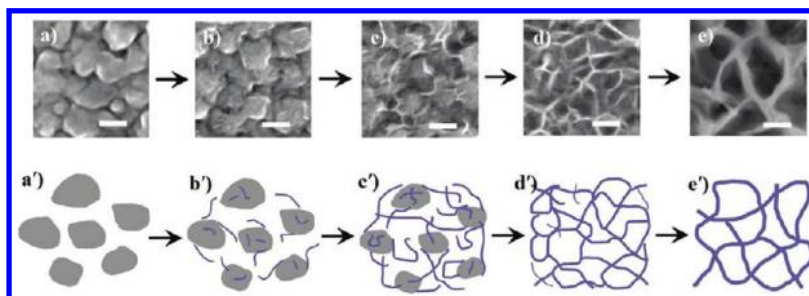
Figure 2. Schematic illustration of the formation and morphology evolution of Ni honeycombs. All the scale bars are 50 nm.

Ni nanostructures are observed on the Al particle surfaces, especially the sites (sharp edges) that have relative greater radius of curvatures (Supporting Information Figure S2c,c'). After 3 h, ridge-like Ni nanostructures grow longer and wider and are interconnected, forming uniform initial honeycomb structure (Supporting Information Figure S2d,d'). After 20 h, multilayers of Ni ridge-like structures can be clearly observed (Supporting Information Figure S2e,e'). Finally, after 2 days, bigger and smooth honeycomb structures with thicker walls are formed on the carbon fiber surface (Supporting Information Figure S2f,f').

A schematic illustration for the evaluation of Ni honeycomb nanostructures, together with the corresponding SEM images, is presented in Figure 2. First, the initial replacement reaction between Al and Ni^{2+} proceeds rapidly, due to the large difference in their redox potentials, Al^{3+}/Al (−1.676 V) and Ni^{2+}/Ni (−0.257 V). This promotes the random formation of Ni nuclear buds and tiny ridge-like structures on selected surface sites (sharp edges that are relatively more active to react with the solution) of Al nanoparticles (Figure 2a–c and a'–c'). The as-formed structures act as the sites for further Ni precipitation, forming longer and wider ridge-like structures that interconnect to form initial honeycomb structures (Figure 2d,d'). With reaction, more and more inner parts of Al nanoparticles participate in the replacement reaction to form new inner honeycomb layers; at the same time, the cells of honeycomb are dug deeper and wider. Note that the continuously produced Ni atoms also precipitate on the surfaces of the as-formed honeycombs. Therefore, with further reorganization of Ni atoms to minimize the surface energy, smooth honeycomb nanostructures with bigger cells and thicker walls are formed finally (Figure 2e,e').

The morphology of the Ni honeycomb can be easily modulated by simply adjusting the experimental parameters. When the Al film thickness was changed from 30 to 100 nm, thicker honeycomb Ni film was formed on the entire carbon paper surface (Figure 3a,b). The average cell size and cell-wall thickness did not change but more layers of honeycomb structures were obtained (Figure 3b vs Figure 1c). We also studied the concentration effect of metal salt precursor on the Ni honeycomb morphology (0.03, 0.1, and 0.5 M $NiCl_2$, with corresponding images shown in Supporting Information Figure S3a,b, S3c,d and S3e,f respectively), while keeping the Al film thickness constant at 30 nm. We found that with the increase of metal salt concentrations, smaller honeycomb cells (from 110, 90 to 60 nm) and thinner wall thickness (from 12, 10, to 8 nm) were obtained. Further, we studied the effect of the different types of metal salt precursors. By substituting the $NiCl_2$ solution with $Ni(NO_3)_2$, slower reaction rate was found, which could be confirmed by the SEM morphology observation of the samples taken from same growth stages. This time, larger honeycombs, in terms of both cell size (~110 nm) and wall thickness (15−20 nm), were formed (Figure 3c,d vs Supporting Information Figure S3c,d and
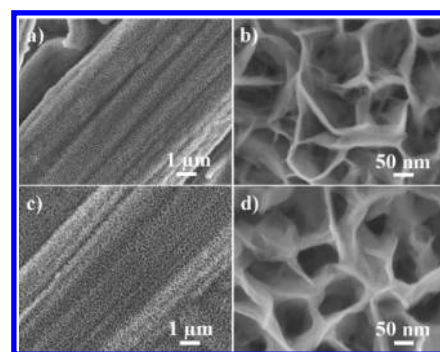

Figure 3. Morphology-controlled synthesis of Ni honeycombs on carbon paper. (a,b) SEM images of the Ni honeycombs synthesized from the reaction of 100 nm Al film on carbon paper and 0.1 M $NiCl_2$ solution. (c,d) SEM images of the Ni honeycombs synthesized from the reaction of 30 nm Al film on carbon paper and 0.1 M $Ni(NO_3)_2$ solution.

Figure 1c). From all of the above, we can conclude that the key factor for the morphological and structural control is the net redox potential between the redox pairs of the sacrificial metal and the target metal to be synthesized. Specifically, with the increase of metal salt concentrations, the net redox potential between the sacrificial metal and the target metal increases; this results in a faster reaction rate to form smaller cells with thinner cell-wall thickness. Another important factor is the anion effect which arises (1) from the influence of the existing anions in solution on the standard redox potential (SRP) of the metal, which affects the reaction rate and then the cell size and wall thickness; and (2) from the differences in anion electronic structures and polar properties, which, to some extent, may affect the aggregation path of the synthesized Ni atoms and, therefore, the final morphology of the metal structure.[30]

To demonstrate the capability of this strategy for the synthesis of other metal nanostructures on substrates, we successfully synthesized Co honeycombs on carbon paper surfaces. In addition, similar systematic morphology-controlled synthesis has also been demonstrated by varying Co salt concentrations and precursors (Supporting Information Figure S4). This reinforces our hypothesis on the key factors that affect the morphologies and structures of the metal nanostructures synthesized via this method. Thus, we believe this method has a great potential in the synthesis of other metal nanostructures on various desired substrates.

Since the discovery of carbon nanotubes (CNTs), they have been widely used as diverse matrices to fabricate various nanocomposites, metal/CNTs, for example, which possess great potential applications in fuel cells, electronic devices, and chemical

(30) Saupe, G. B.; Waraksa, C. C.; Kim, H.; Han, Y. J.; Kaschak, D. M.; Skinner, D. M.; Mallouk, T. E. *Chem. Mater.* **2000**, *12*, 1556–1562.
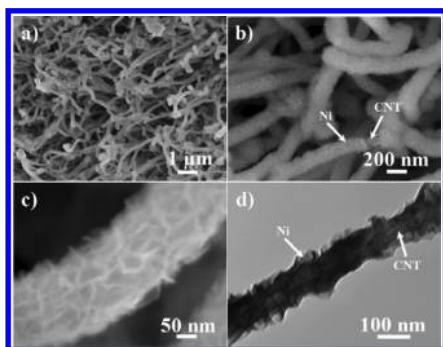
Figure 4. Ni honeycombs synthesized on CNTs. (a,b,c) SEM images at different magnifications and (d) TEM image of CNT@Ni honeycomb core/shell structures, synthesized from 30 nm Al on CNTs and 0.1 M NiCl$_2$ solution.

Figure 5. Ni honeycombs on silicon wafers, synthesized from 30 nm Al film and 0.1 M NiCl$_2$ solution: (a,b) without patterning and (c,d) with square patterning. The inset in (d) shows an enlarged image of a squared pattern of Ni honeycombs.

Figure 6. Schematic illustration of the major steps for generating Al patterns on Si substrate as well as the coating of Al film on Cu grid.

sensors.[31−33] In recent years, our group has achieved experience in the controlled synthesis of CNTs on carbon papers, forming 3D open structures, which can be used as excellent substrate candidates for supporting various nanomaterials for fuel cell applications.[34−36] Here, to demonstrate the utility of our strategy, we have successfully synthesized Ni nanohoneycombs on our in-house synthesized CNTs (Figure 4). We see all the CNT surface has been covered by Ni honeycombs, forming very beautiful, furry, and chubby feather-duster-like CNT@Ni core−shell nanostructures. The CNT cores are about 60 nm in diameter, while the honeycomb shells are about 30−50 nm in thickness. Such CNT@Ni composite core−shell structures that possess high surface/volume ratios are expected to have applications in fuel cells, sensors, and energy storage devices.[37,38]

Silicon has been used in many industrial applications, as it is the principal component of most semiconductor devices, most importantly, integrated circuits or microchips.[39,40] Thus, the fabrication of metal nanostructures on silicon substrate will inevitably enrich their applications in many fields. Here, we have successfully synthesized very uniform Ni honeycombs on a silicon wafer substrate (Figure 5a,b), via the reaction of 30 nm Al film and 0.1 M NiCl$_2$ solution. Neither bumps nor waves were formed on the surface owing to the perfectly smooth surface of the pristine Si wafer. The honeycombs maintained the same size, 80−100 nm in diameter and 10 nm cell-wall thickness, as those synthesized under the same experimental conditions on a carbon paper surface. These metal−Si composites hold great potential in electronics. In recent years, metal thin film patterning is of much technological significance and interest because modern electronic and opto-electronic devices commonly require electrode or metallization patterns.[26−29] Thus, we experimentally synthesized square
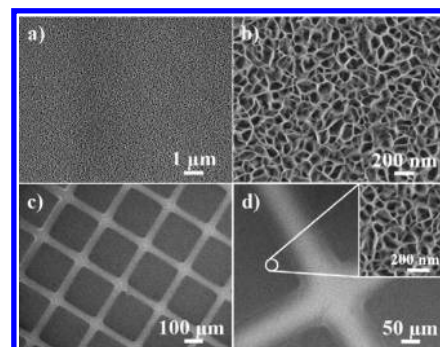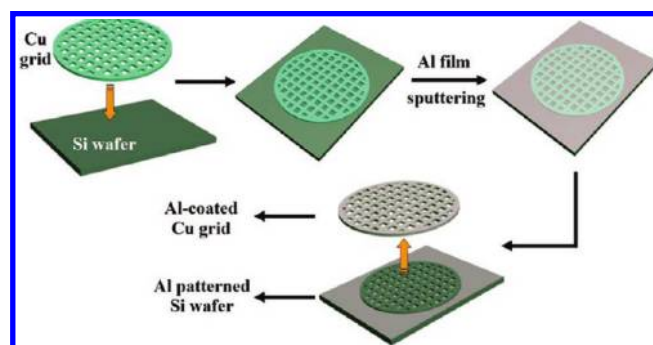
(31) Yang, D. Q.; Sun, S. H.; Sacher, E.; Dodelet, J. P. *J. Phys. Chem. C* **2008**, *112*, 11717−11721.
(32) Baughman, R. H.; Zakhidov, A. A.; de Heer, W. A. *Science* **2002**, *297*, 787−792.
(33) Brahim, S.; Colbern, S.; Gump, R.; Grigorian, L. *J. Appl. Phys.* **2008**, *104*, 024502.
(34) Saha, M. S.; Li, R.; Sun, X. *J. Power Sources* **2008**, *177*, 314−322.
(35) Liu, H.; Zhang, Y.; Arato, D.; Li, R.; Mérel, P.; Sun, X. *Surf. Coat. Technol.* **2008**, *202*, 4114−4120.
(36) Saha, M. S.; Li, R.; Sun, X.; Ye, S. Y. *Electrochem. Commun.* **2009**, *177*, 438−441.
(37) Ayala, P.; Freire, F. L., Jr.; Gu, L.; Smith, D. J.; Solórzano, I. G.; Macedo, D. W.; Vander Sande, J. B.; Terrones, H.; Rodriguez-Manzo, J.; Terrones, M. *Chem. Phys. Lett.* **2006**, *431*, 104−109.
(38) Bittencourt, C.; Felten, A.; Ghijsen, J.; Pireaux, J. J.; Drube, W.; Erni, R.; Van Tendeloo, G. *Chem. Phys. Lett.* **2007**, *436*, 368−372.
(39) Xiang, J.; Lu, W.; Hu, Y.; Wu, Y.; Yan, H.; Lieber, C. M. *Nature* **2006**, *441*, 489−493.
(40) Kim, D.; Ahn, J.; Choi, W. M.; Kim, H.; Kim, T.; Song, J.; Huang, Y. Y.; Liu, Z.; Lu, C.; Rogers, J. A. *Science* **2008**, *320*, 507−511.
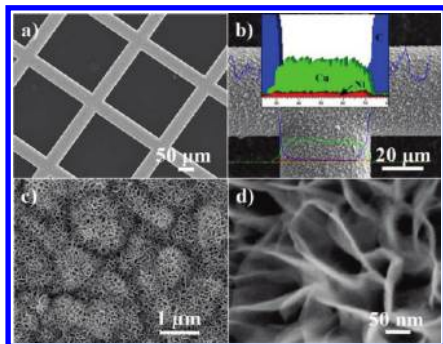
patterned Ni honeycombs on a Si wafer surface, based on a preformed square patterned Al film fabricated via a masking method. The schematic illustration (Figure 6) shows the major steps for generating square Al patterns on a Si substrate surface. First, a Cu grid, acting as a sputtering mask, was tightly bonded on the Si substrate surface. Second, a certain thickness Al film (e.g., 30 nm) was sputtered on the substrate. Third, the Cu grid was carefully peeled off from the Si substrate. Then, the Si wafer with Al film patterns was immersed in the 0.1 M NiCl$_2$ solution for two days. Finally, very uniform, regular square patterned Ni honeycombs were obtained on the Si substrate (Figure 5c,d). The inset in Figure 5d shows a high-magnification image of one of the square Ni patterns. Very uniform Ni honeycombs were obtained, with similar sizes to those reported in Figure 5b. In addition, by immersing the Cu grid that was peeled off from the Si wafer, Ni honeycomb structures on Cu grid were easily obtained (Figure 7), which, to some extent, indicates the efficacy of this strategy for the synthesis of metal−substrate composites. This time, the Ni honeycombs on the Cu grid were not as uniform and flat as that on Si wafer due to the rough pristine surface of the former. However, still the Ni honeycombs undulate along the roughness of Cu grid surface, giving an illusion of decorating flowers on the Cu surfaces. The EDX line scan profile shows the elemental distribution (Ni, Cu, and C) of the Ni honeycombs on Cu grid (Figure 7b), where the C signal came from the colloidal graphite coating on the SEM holder which serves as the substrate background.

Comparing the honeycombs obtained under same experimental conditions, on carbon paper, Si wafer, and Cu grid, we see that they maintain almost the same sizes, 80−100 nm in diameter and 10 nm cell-wall thickness, while the honeycombs on the CNTs

Figure 7. Ni honeycombs synthesized on Cu grid. SEM images at different magnifications. The EDX line scan profile along the horizontal line is indicated in (b).

have smaller sizes, 40−60 nm in diameter and 7 nm cell-wall thickness. This indicates that the nanostructures synthesized via this strategy are highly dependent on the net redox potential between the redox pairs of the sacrificial metal and the target metal to be synthesized (Figures 1,5,7), as well as the type and concentration of the metal salt precursor. (Figures 1,3 and Supporting Information Figure S3). Interestingly, when the substrates are down to nanoscale size, for example, CNTs, their size and shape will play an important role in the formation of the desired metal nanostructures.[41]

4. Conclusions

In conclusion, we have reported a two-step process for the growth of Ni honeycomb nanostructures on various substrates, with and without patterning, via the combination of a

sputter-coating/patterning technique and a replacement reaction solution method. Through a time-dependent morphological evolution study, the growth process of honeycomb nanostructures has been investigated. It has been demonstrated that this strategy is remarkably straightforward and versatile to generate metal nanostructures, with high surface areas and structural uniformity, on various substrates. In addition, this approach allows stepwise control and optimization of experimental conditions, providing an opportunity for rational design and synthesis of controlled architectures at the nanoscale. The easy success of the morphology controlled synthesis of Co metal nanostructures on substrates indicates the great potential of this strategy in the synthesis of other metal nanostructures on various desired substrates. In short, the central innovation here is that a simple and cost-effective means for producing metal nanostructures on various desired substrates has been reported, and the technique may have great technological impact. These metal−substrate composites, especially with desired patterns, are expected to be ideal candidates to be used in modern electronic and optoelectronic devices, sensors, fuel cells, and energy storage systems.

Supporting Information Available: EDX spectrum of Ni honeycombs on carbon paper; SEM images of the morphological evolution of Ni honeycombs as a function of reaction time; and SEM images of the morphology controlled syntheses of Ni and Co honeycombs. This material is available free of charge via the Internet at http://pubs.acs.org.

(41) Brege, J. J.; Hamilton, C. E.; Crouse, C. A.; Barron, A. R. *Nano Lett.* **2009**, *9*, 2239–2242.